Excitons in rolled up nanotubes of type-II semiconductor quantum wells: Theoretical study of a quasi-one-dimensional bosonic gas

Mehran Bagheri* and Farshad Ebrahimi†
Department of Physics, Shahid Beheshti University, Evin, Tehran 19839, Iran
(Received 16 January 2008; revised manuscript received 28 April 2008; published 15 July 2008)

The excitonic states and the quantum degenerate excitonic gas of spatially separated electron hole in an ideal rolled up nanotube of type-II semiconductor quantum wells with reverse bias configuration are studied theoretically. To illustrate the situation using the material constants appropriate to GaAs/AlAs type-II semiconductor, the exciton binding energy, its ground-state wave function, and the energies of the two low lying rotational states are calculated by numerical diagonalization of the single electron-hole Hamiltonian. By exploiting the ground-state wave function, the exciton-exciton interaction potential in the low-density limit is evaluated and found to be repulsive. It is then shown that a gas of such excitons at low temperature below the energies of the low lying rotational states behaves as a quasi-one-dimensional bosonic gas, which, at low density, is in the strong-coupling regime, and the excitons become fermions and the orthoexcitonic gas is paramagnetic.

DOI: 10.1103/PhysRevB.78.045312 PACS number(s): 73.21.−b, 05.30.Jp, 71.35.Lk

I. INTRODUCTION

Since the first experimental observation of the Bose-Einstein condensation (BEC) in a weakly interacting sample of ultracold trapped gases of alkali atoms,[1] the subject of a degenerate system of bosons, i.e., the bosonic quantum liquid, has evolved to be a field of very active research in both atomic and condensed-matter physics.[2,3] Such liquid would exhibit a quantum condensate in which a macroscopic number of either single particles or of pairs of particles are condensed into the same quantum state.[4] The quest for the realization of BEC in other systems such as excitons,[3,5–7] exciton polaritons in semiconductor microcavities,[8–10] magnons,[11] and Hall bilayers[12] is still actively pursued with no conclusive evidence. Exciton and polariton BECs are the most promising candidates, following early suggestions of possible excitonic BEC proposed by Moskalenko,[13] Blatt *et al.*,[14] and Keldysh and Koslov[15] in the 1960s. The strong Coulomb-correlated pair of electron and hole, which is an exciton, in a semiconductor behaves like a boson and a gas of excitons is expected to undergo BEC under appropriate circumstances. Due to their light masses, excitons transform into quantum condensate at a temperature several orders of magnitude higher than for atomic gases.[8,9]

A very large number of studies have been devoted to the possible condensation of excitons in different types of bulk semiconductors.[3,16–20] Contrary to the infinite lifetime of atomic gases, in such systems, difficulty originates from the short excitonic lifetime, which can range from a few picoseconds to microseconds. This prevents sufficient number of excitons to build up a condensed ordered phase. One way to overcome this difficulty is to exploit a two-dimensional system of spatially separated electron hole (SSEH) pairs, which are indirect excitons that allows the realization of a long-lived exciton gas. There have been several claims of the excitonic condensation of indirect excitons in coupled quantum wells (QWs).[6,21–26] In such systems, interacting electrons and holes are restricted to move in separated lower dimensional structures. In fact, since the pioneering works in Refs. 27–32 over the past four decades, designing and creating new types of SSEH devices for investigating various possible low-temperature collective phases such as BEC, Mott transition, and the coherent BCS-type state of *e-h* pairs have received tremendous attentions.

In this paper we propose an ideal rolled up type-II semiconductor QW with reverse bias configuration in which electrons and holes are spatially separated in two concentric cylindrical tubes by the applied voltage (see Fig. 1). The motivation of this work is to create a quasi-one-dimensional (1D) bosonic gas of excitons (para or ortho) based on curved SSEH layers and to investigate its properties. Owing to the advancement of semiconductor nanotechnology, it is becoming possible to fabricate such curved two-dimensional systems where the electrons and holes are close enough to interact strongly while tolerably separated from others to prevent tunneling and optical recombination.[33] Some early works[34] have also shown that in spatially separated excitonic systems when the charge separation between the electrons and holes within a single exciton in low-dimensional structures is large enough, the interaction between indirect excitons are completely repulsive so that the exciton gas is stable against collapse.

The paper is organized as follow. In Sec. II, we adopt an ideal type-II semiconductor QW nanotube in reverse bias configuration based on the GaAs/AlAs material properties[35,36] where, because of reverse biasing, the electrons are restricted to move on the outer tube, and the holes over the inner one and the center of mass of the exciton has translational motion along the tube axis. We establish the single exciton Hamiltonian and calculate its low lying spectrum. In Sec. III, using the aforesaid single exciton wave functions, the exciton-exciton interaction is evaluated and found to be repulsive. This repulsive interaction between the excitons is helpful to stabilize the exciton state against establishment of exciton molecules and for the formation of quasi-1D repulsive bosonic gas. Finally, in Sec. IV, by mapping the exciton gas onto a quasi-1D bosonic gas interacting via the delta-function potential, we discuss the properties of the quasi-1D bosonic gas of excitons at the low-temperature and low-density limit.

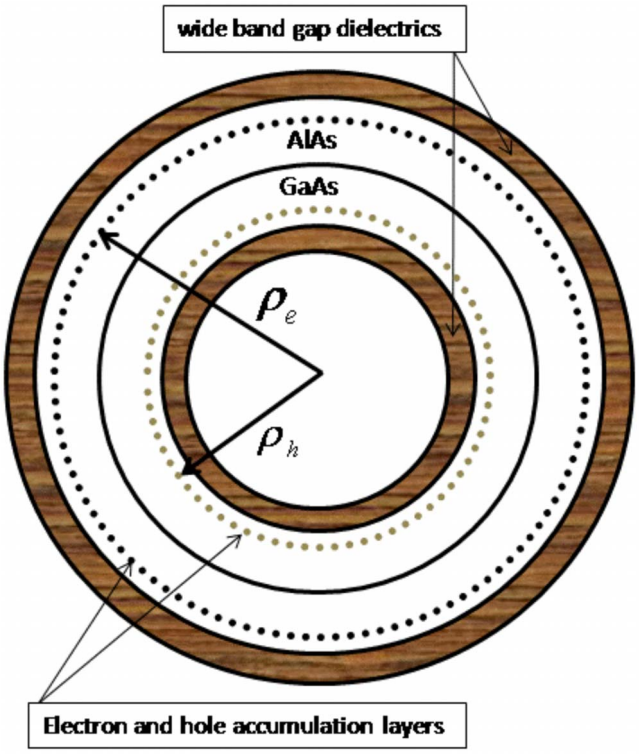

FIG. 1. (Color online) Cross section of an ideal rolled up semiconductor QW nanotube of GaAs/AlAs. The outer and inner tubes are wide band-gap dielectrics; the dotted circles adjacent to the dielectric layers are the electron and hole accumulation layers. The structure is in reverse bias configuration. For the numerical calculation, we have assumed $\rho_h = 25a^* \simeq 600$ Å, and the separation of the electron and hole accumulation layers to be $d = |\rho_e - \rho_h| = 1.5a^* \simeq 36$ Å.

II. MODEL AND APPROACH

As depicted in Fig. 1, we address a model consisting of a rolled up type-II semiconductor QW nanotube in which by reverse biasing the electrons and holes, accumulate and move over the outer and inner tubular shells close to the outer and inner dielectric layers, respectively. As a model, we assume that the electrons and holes are strongly confined in the radial direction close to the dielectric layers by the applied reverse bias voltage. Consequently, the effective thickness of each accumulation layer is assumed to be very narrow. This assumption implies that the wave-function spread for both electrons and holes in the radial direction is negligible. In this model, contrary to the case of single-wall nanotube, the electron and hole wave functions cannot overlap and they can only interact via their Coulomb attraction, and the electron-hole exchange term is zero.[3] Also, due to spatial separation of electron and hole in double-wall nanotube, the excitons have permanent electric multipole fields. For simplicity, we assume the thicknesses of the accumulation layers to be zero. Furthermore, we only consider the low-density limit. In this limit, the screening, due to other electrons and holes on the Coulomb attraction between electron and hole of an exciton, can be neglected.

For electron and hole masses, we choose the parameters of GaAs/AlAs: $m^*_{e_z} = 1.1m_e$, $m^*_{e_{xy}} = 0.19m_e$, and $m^*_{h_z} = m^*_{h_{xy}} = 0.37m_e$, where m_e is the free-electron mass.[34,35] Using cylindrical coordinates, $\vec{x}_i = (\rho_i, \varphi_i, z_i)$,[37] where the indices $i = h, e$ correspond to the hole and electron, and ρ_h and ρ_e $(\rho_h < \rho_e)$ are the radii of the tubular shells of the accumulated holes and electrons, respectively. The Hamiltonian describing the dynamic of electron and hole in the effective-mass approximation is given by

$$\hat{\mathcal{H}} = -\frac{\hbar^2}{2m^*_{e_{xy}}\rho_e^2}\frac{\partial^2}{\partial\varphi_e^2} - \frac{\hbar^2}{2m^*_{e_z}}\frac{\partial^2}{\partial z_e^2} - \frac{\hbar^2}{2m^*_{h_{xy}}\rho_h^2}\frac{\partial^2}{\partial\varphi_h^2} - \frac{\hbar^2}{2m^*_{h_z}}\frac{\partial^2}{\partial z_h^2} - \frac{e^2}{\varepsilon[\rho_e^2 + \rho_h^2 - 2\rho_e\rho_h\cos(\varphi_e - \varphi_h) + (z_e - z_h)^2]^{1/2}}, \quad (1)$$

in which the first and the second terms are, respectively, kinetic energies of the electron and hole, and the last term is the Coulomb potential, e is the electron charge, and $\varepsilon = 12.53$ is the dielectric constant of the nanotube. It is now convenient to separate the motion of the two particles in the z direction into that of the center of mass of the exciton and its relative motion. The exciton wave function may then be written as

$$\Psi(z_{\rm cm}; z_{\rm rel}, \varphi_e, \varphi_h) = \psi(z_{\rm rel}, \varphi_e, \varphi_h)\phi_{\mathbf{k}}(z_{\rm cm}), \quad (2)$$

where $\phi_{\mathbf{k}}(z_{\rm cm}) = 1/\sqrt{2\pi}e^{i\mathbf{k}z_{\rm cm}}$ is the wave function of the center of mass and $\psi(z_{\rm rel}, \varphi_e, \varphi_h)$ is the relative wave function of the exciton. As a consequence of the axial symmetry of the nanotube, the total angular momentum of the exciton, $L_z = L_{z_e} + L_{z_h}$, is conserved and there is no coupling between the eigenfunctions with different values of the total angular momentum. Therefore, it is convenient to expand the relative eigenfunctions of the exciton in terms of the normalized eigenfunctions of the L_z, $[(1/2\pi)e^{i(l_1\varphi_e + l_2\varphi_h)}]$. If we denote the relative eigenfunctions of the exciton by ψ_l^n in the eigenfunction basis of L_z, they can be written as

$$\psi_l^n(z_{\rm rel}, \varphi_e, \varphi_h) = \left(\frac{1}{2\pi}\right)\sum_{\substack{l_1, l_2 = -\infty \\ l = l_1 + l_2}}^{\infty} f^n_{l_1,l_2}(z_{\rm rel})e^{-i(l_1\varphi_e + l_2\varphi_h)}, \quad (3)$$

where $l = l_1 + l_2$ is the quantum number of the total orbital angular momentum of the exciton and n is its principle quantum number. The functions $f^n_{l_1,l_2}(z_{\rm rel})$ in Eq. (3) depend on the relative coordinate of the electron and hole in the z direction, and they obey the following coupled-channel Schrödinger's equation,

$$-\frac{d^2}{dz_{\rm rel}^2}f^n_{l_1,l_2}(z_{\rm rel}) + \sum_{m=-\infty}^{\infty} V^m_{l_1,l_2}(z_{\rm rel})f^n_{l_1+m,l_2-m}(z_{\rm rel}) = \mathcal{E}^n_l f^n_{l_1,l_2}(z_{\rm rel}); \quad l = l_1 + l_2, \quad (4)$$

for $l = 0, \pm 1, \pm 2, \ldots$ and $n = 0, 1, 2, \ldots$. The transformation of the Hamiltonian [Eq. (1)] to the center of mass with their associated variables, and the functional form of $V^m_{l_1,l_2}$ and their graphs are presented in Appendix A

Since we are interested in obtaining low lying bound states of the exciton, we numerically solve the system of Eq. (4) with boundary conditions $f^n_{l_1,l_2}(-\infty) = f^n_{l_1,l_2}(\infty) = 0$. For this purpose, we have exploited the FDEXTR code based on the

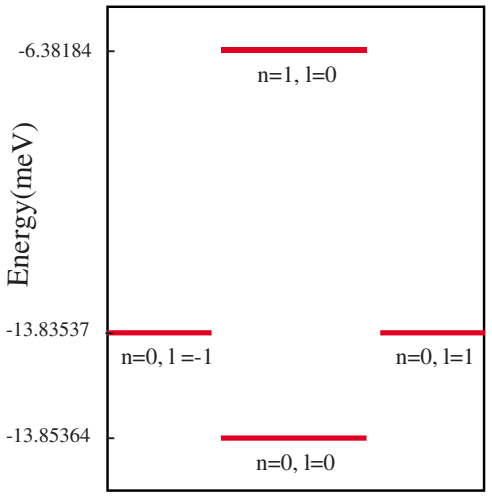

FIG. 2. (Color online) The energy diagram for $(n=0,l=0)$, $(n=0,l=\pm 1)$, and $(n=1,l=0)$ states of the exciton in rolled up nanotube of GaAs/AlAs QW with $\rho_h=25a^*$, $\rho_e=26.5a^*$, and $d=1.5a^*$.

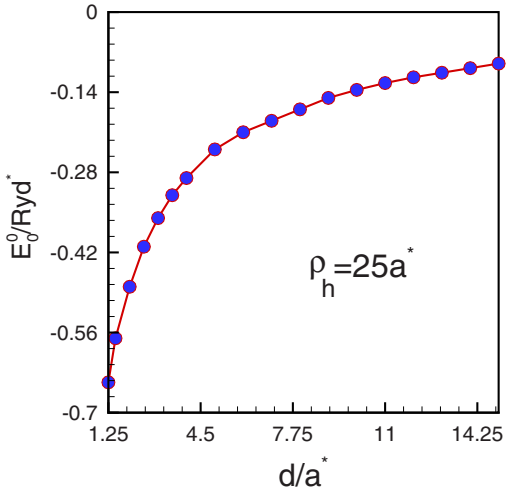

FIG. 3. (Color online) The exciton ground-state energy $\mathcal{E}_0^0$ as a function of 18 values of the separation of the electron and hole layers.

Richardson extrapolation.[38] The systems of coupled equations are solved for a fixed value of l. For example, the case $l_2=-l_1$ corresponds to zero total angular momentum $l=0$. So, we have to solve a system of coupled equations for each value of the total angular momentum l separately. For our objective, we run the code with the configuration of Fig. 1 for $l=0$ and $l=\pm 1$ with 105 and 106 channels, respectively. Increasing the number of channels leaves the results practically unchanged up to 10^{-5}. As depicted in Fig. 2, the ground-state energy for the cases $l=0$ and $l=\pm 1$, i.e., $\mathcal{E}_{l=0}^0$ and $\mathcal{E}_{l=\pm 1}^0$, are −13.85364 and −13.83537 meV, respectively. We have also calculated the first-excited-state energy for the case $l=0$. For the binding energy of this state, we obtained the value of −6.38184 meV. Furthermore, in Fig. 3, we have presented the calculated exciton ground-state energy as a function of the separation of the electron and hole layers. In Fig. 4, panels (a) and (b) show the first five smallest and the first five largest terms of the expansion of the ground-state wave function of the exciton, respectively. As shown, the dominant contribution comes from the component $f_{0,0}^0$. The size of the exciton, which is related to the e-h interaction, can be determined from the width of the ground-state probability distribution. Figure 5 exhibits the ground-state probability distribution of the exciton along the z_{rel} direction. Finally, we have calculated the mean quadratic e-h separation, $a=\langle z_{\mathrm{rel}}^2\rangle^{1/2}$, which gives an idea of the size of the exciton. It is found to be ~41.52 Å.

III. EXCITON-EXCITON INTERACTION

Since we are interested in the bosonic properties of spatially separated excitonic gas in rolled up nanotube of GaAs/AlAs QW, we consider the low density limit set by the condition, $n_{1D}a \ll 1$, where n_{1D} is the linear density of the gas and a is the size of the exciton. This is the density range where the interparticle spacing, n_{1D}^{-1}, is much larger than the size of the exciton, a. In this range of density, the excitons will act as bosons and the Bose properties of excitons dominate the behavior of the gas.

The Hamiltonian of such a bosonic gas consists of the energy of the relative motion of electrons and holes, the kinetic energy of the translational motion of the center of mass of the excitons, and the sum of the exciton-exciton interactions. In terms of second-quantized bosonic field operators $\hat{\Psi}(z_{cm};z_{\mathrm{rel}},\varphi_e,\varphi_h)$, the first two parts of the Hamiltonian can be written as[39]

$$\hat{\mathcal{H}}_1 = \int_{-\infty}^{\infty}\int_{-\infty}^{\infty}\int_0^{2\pi}\int_0^{2\pi} dz_{\mathrm{cm}}dz_{\mathrm{rel}}d\varphi_e d\varphi_h \hat{\Psi}^\dagger(z_{\mathrm{cm}};z_{\mathrm{rel}},\varphi_e,\varphi_h) \times \left[-\frac{\hbar^2}{2M^*}\frac{\partial^2}{\partial z_{\mathrm{cm}}^2} + \hat{\mathcal{H}}_{\mathrm{rel}}\right]\hat{\Psi}(z_{\mathrm{cm}};z_{\mathrm{rel}},\varphi_e,\varphi_h). \quad (5)$$

The contribution of the exciton-exciton interactions to the Hamiltonian of the exciton gas has two parts: one from the direct Coulomb interactions between electrons and holes of different excitons, which has the form

$$\hat{\mathcal{H}}_2 = \frac{1}{2}\int_{-\infty}^{\infty}\int_{-\infty}^{\infty}\int_{-\infty}^{\infty}\int_{-\infty}^{\infty}\int_0^{2\pi}\int_0^{2\pi}\int_0^{2\pi}\int_0^{2\pi} dz_{\mathrm{cm}_1}dz_{\mathrm{cm}_2}dz_{\mathrm{rel}_1}dz_{\mathrm{rel}_2}d\varphi_{e_1}d\varphi_{e_2}d\varphi_{h_1}d\varphi_{h_2}$$
$$\times \hat{\Psi}^\dagger(z_{\mathrm{cm}_1};z_{\mathrm{rel}_1},\varphi_{e_1},\varphi_{h_1})\hat{\Psi}^\dagger(z_{\mathrm{cm}_2};z_{\mathrm{rel}_2},\varphi_{e_2},\varphi_{h_2}) \times [V(\vec{x}_{e_1},\vec{x}_{e_2}) + V(\vec{x}_{h_1},\vec{x}_{h_2}) + V(\vec{x}_{e_1},\vec{x}_{h_2}) + V(\vec{x}_{e_2},\vec{x}_{h_1})]$$
$$\times \hat{\Psi}(z_{\mathrm{cm}_2};z_{\mathrm{rel}_2},\varphi_{e_2},\varphi_{h_2})\hat{\Psi}(z_{\mathrm{cm}_1};z_{\mathrm{rel}_1},\varphi_{e_1},\varphi_{h_1}). \quad (6)$$

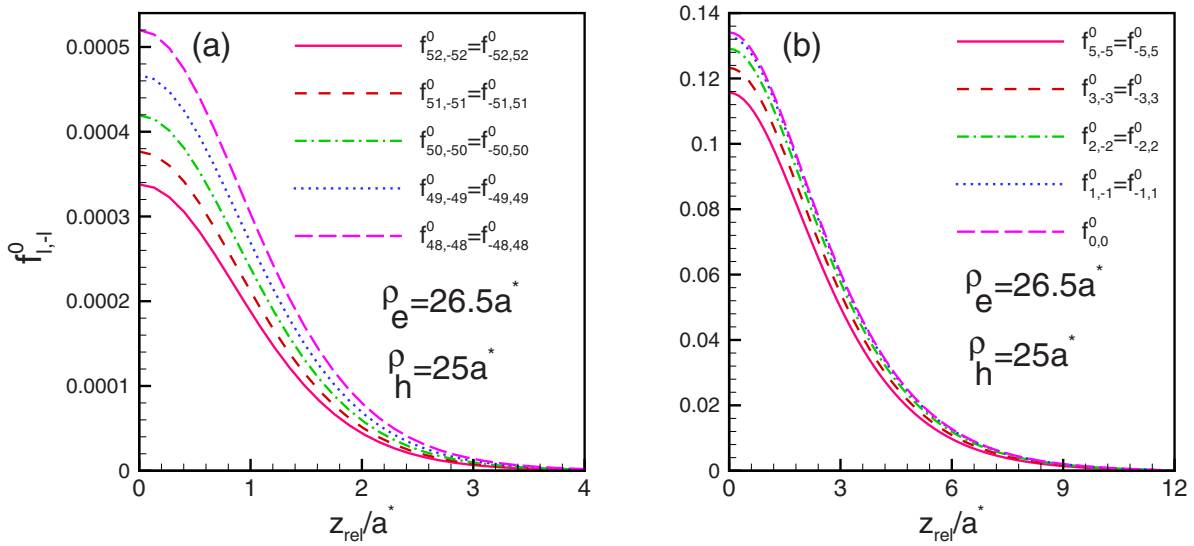

FIG. 4. (Color online) The (a) five smallest and the (b) five largest terms of the ground-state exciton wave function as functions of the electron-hole separation z_{rel}.

and a part from the Coulomb exchange effect. We will show that in our model, due to the repulsive force between excitons, this term is small and can be dropped from the Hamiltonian.

Since we are interested in the excitonic states of electron hole, we expand the field operator $\hat{\Psi}(z_{\mathrm{cm}};z_{\mathrm{rel}},\varphi_e,\varphi_h)$ in terms of the center-of-mass wave functions, $\{\phi_{\mathbf{k}}(z_{\mathrm{cm}})\}$, and excitonic eigenfunctions, $\{\psi_l^n(z_{\mathrm{rel}},\varphi_e,\varphi_h)\}$,

$$\hat{\Psi}(z_{\mathrm{cm}};z_{\mathrm{rel}},\varphi_e,\varphi_h)=\sum_{n=0}^{\infty}\sum_{l=-\infty}^{\infty}\sum_{\mathbf{k}}\hat{b}_l^n(\mathbf{k})\phi_{\mathbf{k}}(z_{\mathrm{cm}})\psi_l^n(z_{\mathrm{rel}},\varphi_e,\varphi_h), \tag{7}$$

where n and l are introduced in Eq. (3), and $\hat{b}_l^n(\mathbf{k})$ is the annihilation operator, which obeys the usual boson commutation relations. For temperatures much lower than the energies of the first-excited rotational states of the exciton, i.e., $n=0$ and $l=\pm 1$, we can approximate the field operator by keeping only the $n=0,l=0$ term in the expansion. This reduces the form of the field operator to

$$\hat{\Psi}(z_{\mathrm{cm}};z_{\mathrm{rel}},\varphi_e,\varphi_h)=\sum_{\mathbf{k}}\hat{b}_0^0(\mathbf{k})\phi_{\mathbf{k}}(z_{\mathrm{cm}})\psi_0^0(z_{\mathrm{rel}},\varphi_e,\varphi_h). \tag{8}$$

Using the above field operator in the total Hamiltonian and defining the bosonic field operator

$$\hat{\Phi}(z_{\mathrm{cm}})=\sum_{\mathbf{k}}\hat{b}_0^0(\mathbf{k})\phi_{\mathbf{k}}(z_{\mathrm{cm}}), \tag{9}$$

which annihilates an exciton when it is in its ground state at point z_{cm}, after integration over the variables z_{rel_1}, z_{rel_2}, φ_e, and φ_h, we obtain the following effective 1D Hamiltonian

$$\hat{\mathcal{H}}_{\mathrm{eff}}=\int_{-\infty}^{\infty}dz_{\mathrm{cm}}\hat{\Phi}^{\dagger}(z_{\mathrm{cm}})\left[-\frac{\hbar^2}{2M^*}\frac{\partial^2}{\partial z_{\mathrm{cm}}^2}-\mathcal{E}_0^0\right]\hat{\Phi}(z_{\mathrm{cm}})+\frac{1}{2}\int_{-\infty}^{\infty}\int_{-\infty}^{\infty}dz_{\mathrm{cm}_1}dz_{\mathrm{cm}_2}\hat{\Phi}^{\dagger}(z_{\mathrm{cm}_1})\hat{\Phi}^{\dagger}(z_{\mathrm{cm}_2})\mathbf{V}(z_{\mathrm{cm}_1}-z_{\mathrm{cm}_2})\hat{\Phi}(z_{\mathrm{cm}_2})\hat{\Phi}(z_{\mathrm{cm}_1}), \tag{10}$$

where $\mathbf{V}(z)$, with $z\equiv(z_{\mathrm{cm}_1}-z_{\mathrm{cm}_2})$, is the interaction potential between two excitons in their ground, state which is the sum of the following four terms

$$\mathbf{V}_i=C_i\int_{-\infty}^{\infty}\int_{-\infty}^{\infty}dz_{\mathrm{rel}_1}dz_{\mathrm{rel}_2}Q_{-1/2}(\chi_i)\sum_{\mu=-52}^{52}\sum_{\mu'=-52}^{52}|f^0_{\mu,-\mu}(z_{\mathrm{rel}_1})|^2|f^0_{\mu',-\mu'}(z_{\mathrm{rel}_2})|^2;\quad i=1,2,3,4, \tag{11}$$

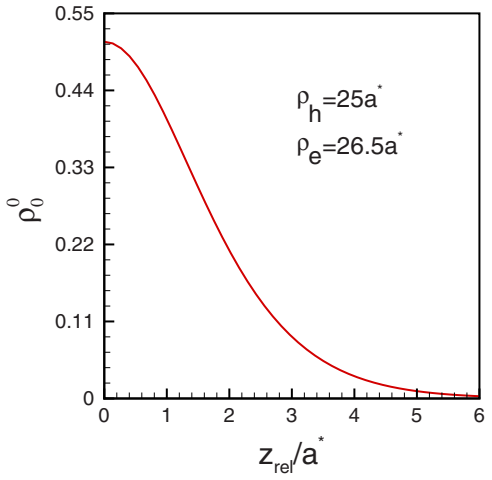

FIG. 5. (Color online) The extent of the ground-state probability density distribution of the exciton along z_{rel}.

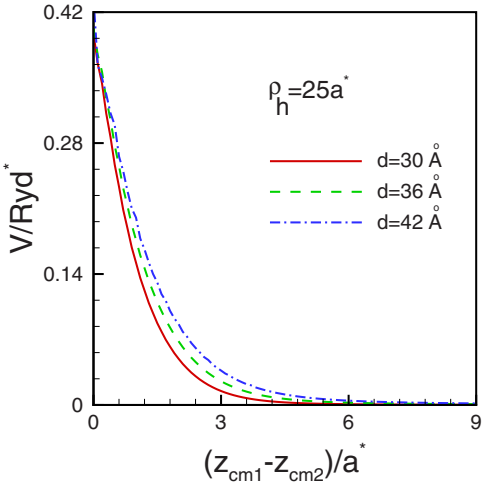

FIG. 6. (Color online) The exciton-exciton interaction potential as a function of the relative distance for three different values of the separation of the electron and hole layers.

where C_i and χ_i for $i=1,2,3,4$ are given in Appendix B. The numerically calculated interaction potential between two excitons for three different thicknesses are plotted in Fig. 6, the interaction is repulsive for all values of z. This can be explained by the effects of the charge separation of excitons imposed by the double-wall geometry of the nanotube, which creates effective electric multipole moments for the excitons. In Appendix B, the lowest-order multipole expansion of the interaction potential between two excitons is derived. In the lowest order, the interaction potential for $\bar{z} \gg \bar{\rho}_e$ has the form $M_{\mathrm{quad}}/|\bar{z}|^5$. This is a repulsive quadrupole interaction with $M_{\mathrm{quad}}=12(m_{e_z}^{*2}-m_{h_z}^{*2})^2\bar{a}^4/M^{*2}+3(\bar{\rho}_e^2-\bar{\rho}_h^2)^2$. The second term is due to the charge separation of excitons, which, for single-wall nanotube, is absent. The absence of dipole term in the interaction potential is owing to the cylindrical symmetry of the nanotube, which averages the dipole term to zero.

The order of exchange interaction between two excitons and its contribution to the total energy of the gas depends on the degree of overlap of wave functions of the excitons, and the density of the gas, respectively. The extent of overlap of the wave functions depends on the penetration probability through the repulsive potential between two excitons. Using the WKB (Ref. 40) approximation, we have calculated the penetration probability through the potential, given by the sum of the four terms in Eq. (11), to a distance of the size of the exciton. For $\rho_h=25a^*$ and $\rho_e=26.5a^*$, and energy of the exciton of the order of its thermal energy for temperature less than 0.2 K, the penetration probability is less than $\sim 8.44 \times 10^{-2}$. So, for the temperature range of our model, the overlaps of the wave functions of the excitons are very small and for the low-density regime, $n_{1D}a \ll 1$, the exchange effects can be neglected.

In the low-density limit, we can approximate the exciton-exciton interaction potential by its s-wave scattering length, $V(z)=g_{1D}\delta(z)$, where $g_{1D}=-\hbar^2/\tilde{\mu}^* a_{1D}$ is the coupling strength in which $\tilde{\mu}^*=M^*/2$ is the reduced mass of two excitons and a_{1D} is the 1D scattering length.[41] The scattering solution of the 1D Schrödinger equation with the relative coordinate z has the general form[42]

$$\tilde{\psi}(z) \sim e^{ikz} + 2e^{ik|z|}\sum_{\nu=0}^{1} ie^{i\delta_\nu}\sin(\delta_\nu)Y_\nu(\hat{z}), \tag{12}$$

where $|k|=\sqrt{2\tilde{\mu}^*\tilde{\mathcal{E}}}/\hbar$, and $Y_\nu(\hat{z})$ and $\nu=0,1$ are 1D spherical harmonics defined as $Y_0(\hat{z})=1/\sqrt{2}$ and $Y_1(\hat{z})=\mathrm{sign}(z)/\sqrt{2}$, and δ_ν are the scattering phase shifts, which for s wave, $\nu=0$, is given by the formula[42]

$$\delta_0(k) = -kR + \arctan\left[-\frac{\gamma_0(k)}{k}\right]. \tag{13}$$

In the above equation, R is the maximum range of the exciton-exciton potential, in which we can choose to comply with the accuracy of the potential ($\sim 10^{-5}$), and γ_0 is the logarithmic derivative of the wave function evaluated at point R. The 1D s-wave scattering length can be determined using the relation[41]

$$a_{1D} = -\lim_{k\to 0}\frac{\partial\delta_0(k)}{\partial k}. \tag{14}$$

For the potential, $\mathbf{V}(z)$, depicted in Fig. 6 ($d=36$ Å) and choosing $R \sim 25a^*$ to comply with the numerical accuracy, we obtain, for the a_{1D}, the value of ~ 86.14 Å. Thus, a gas of SSEH excitons in a rolled up nanotube of GaAs/AlAs QW at low enough temperatures and low enough densities behaves as a quasi-1D bosonic gas with repulsive delta-function potential.

IV. RESULTS AND CONCLUSION

We now investigate the prospect of reaching the quantum degeneracy in the SSEH excitonic gas in the rolled up nanotube of GaAs/AlAs semiconductor QW. We start by briefly reviewing the properties of an interacting 1D Bose gas in the thermodynamic limit.

For a 1D Bose gas with repulsive delta-function potential

with the coupling strength, g_{1D}, linear gas density, n_{1D}, and particle mass, M^*, the dimensionless coupling parameter is $\gamma = M^* g_{1D}/2\hbar^2 n_{1D}$. In the weak-coupling limit, i.e., when $\gamma \ll 1$, for temperatures between the quantum degeneracy temperature, $T_d = \hbar^2 n_{1D}^2/2M^* k_B$, and $\sqrt{\gamma} T_d$, the gas is in the fully decoherence regime. For temperatures less than $\sqrt{\gamma} T_d$, the gas enters the quasicondensate state, which is a Bose condensate state with fluctuating phase. In the strong-coupling regime (Tonks-Girardeau regime[43]), $\gamma \gg 1$, the phenomena of fermionization happens. In this regime due to the strong repulsive potential between the bosons, the wave function of the gas must be antisymmetric with respect to the space variables of the particles. In this regime, the boson gas behaves like a free fermion gas both below and above the degeneracy temperature.[44]

For the SSEH exciton gas presented in the previous section, at temperatures less than $|\mathcal{E}^0_{l=\pm 1} - \mathcal{E}^0_{l=0}|/k_B$, only the ground state of the exciton is relevant and the exciton gas can be considered as a single-component quasi-1D Bose gas. This temperature for our model is 0.2 K. The quantum degeneracy limit is reached when the thermal de-Broglie wavelength, $\lambda_T = (2\pi\hbar^2/M^* k_B T)^{1/2}$, becomes comparable with the interparticle spacing, n_{1D}^{-1}, i.e., when we have $n_{1D}\lambda_T \sim 1$. This happens at temperature equal to T_d. At low densities when $n_{1D} a_{1D} \ll 1$, the SSEH exciton gas in our model has a repulsive delta-function potential. If we choose the linear densities of electrons and holes to be about $n_{1D} = 5 \times 10^4$ cm^{-1}, the degeneracy temperature is $T_d \sim 7.42$ mK with $a_{1D} = 86.14$ Å, the coupling constant is $g_{1D} \sim 121$ meV Å, and the above condition for the s-wave approximation is well satisfied, and the exciton gas in the nanotube is in the strong-coupling regime with $\gamma \sim 48$. In this regime the excitons become fermions with respect to their space variables, both below and above the degeneracy temperature, and the ground state of the gas has a 1D Fermi-Dirac distribution with each state being occupied with only one exciton regardless of its spin state. Thus, a gas of orthoexcitons, $s=1$, in this regime is paramagnetic.[44] Furthermore, for all the excitons to become fermionic, it is also necessary that the Fermi energy of the gas be less than $|\mathcal{E}^0_{l=\pm 1} - \mathcal{E}^0_{l=0}|$ or $n_{1D} < \sqrt{2M^*|\mathcal{E}^0_{l=\pm 1} - \mathcal{E}^0_{l=0}|/\pi^2\hbar^2}$ to prevent transition to the $l = \pm 1$ rotational states of the exciton where, for $n_{1D} = 5 \times 10^4$ cm^{-1}, this condition is also fulfilled.

ACKNOWLEDGMENTS

M.B. is most thankful to Liviu Gr. Ixaru for assisting and providing some initial numerical results on multichannel Schrödinger's equation.

APPENDIX A

In this appendix we present the transformation to the center of mass and relative coordinates of the exciton. We utilize $z_{\rm cm} = (m^*_{e_z} z_e + m^*_{h_z} z_h)/(m^*_{e_z} + m^*_{h_z})$ and its relative coordinate, $z_{\rm rel} = z_e - z_h$, in the z direction, thereby introducing the total mass $M^* = m^*_{e_z} + m^*_{h_z}$ and the reduced mass $\mu^* = m^*_{e_z} m^*_{h_z}/M^*$. Therefore, the total Hamiltonian of the exciton can be written as follows:

$$\hat{\mathcal{H}} = \hat{\mathcal{H}}_{\rm cm} + \hat{\mathcal{H}}_{\rm rel}, \tag{A1}$$

in which

$$\hat{\mathcal{H}}_{\rm cm} = -\frac{\hbar^2}{2M^*}\frac{\partial^2}{\partial z_{\rm cm}^2}, \tag{A2}$$

and

$$\hat{\mathcal{H}}_{\rm rel} = -\frac{\hbar^2}{2\mu^*}\frac{\partial^2}{\partial z_{\rm rel}^2} - \frac{\hbar^2}{2I_e}\frac{\partial^2}{\partial \varphi_e^2} - \frac{\hbar^2}{2I_h}\frac{\partial^2}{\partial \varphi_h^2} - \frac{e^2}{\varepsilon[\rho_e^2 + \rho_h^2 - 2\rho_e\rho_h\cos(\varphi_e - \varphi_h) + z_{\rm rel}^2]^{1/2}}, \tag{A3}$$

where $I_e = m^*_{e_{xy}}\rho_e^2$ and $I_h = m^*_{h_{xy}}\rho_h^2$ are the electron and hole moment of inertia, respectively. For determining the eigenfunctions and eigenvalues of the relative Hamiltonian, it is desirable to expand the Coulomb interaction potential in terms of the angular functions as follows:[45]

$$-\frac{e^2}{\varepsilon[\rho_e^2 + \rho_h^2 - 2\rho_e\rho_h\cos(\varphi_e - \varphi_h) + z_{\rm rel}^2]^{1/2}} = -\frac{e^2}{\pi\varepsilon\sqrt{\rho_e\rho_h}}\sum_{m=-\infty}^{\infty} e^{im(\varphi_e - \varphi_h)} Q_{|m|-1/2}(\chi), \tag{A4}$$

where $Q_{|m|-1/2}$ is the half-integer degree Legendre function of the second kind with $\chi \equiv [\rho_e^2 + \rho_h^2 + z_{\rm rel}^2]/(2\rho_e\rho_h)$. Using the effective Bohr radius $a^* = \varepsilon\hbar^2/\mu^* e^2 \simeq 24$ Å and the effective Rydberg energy $\mathrm{Ryd}^* = \hbar^2/2\mu^* a^{*2} \simeq 24$ meV as units of length and energy, respectively, we define the dimensionless coordinate $\bar{z}_{\rm rel} = z_{\rm rel}/a^*$ and the dimensionless energy $\bar{\mathcal{E}} = \mathcal{E}/\mathrm{Ryd}^*$. Thus, the relative wave function of the exciton meets Schrödinger's equation as follows:

$$[\hat{\mathcal{H}}_{\rm rel} - \hat{I}\bar{\mathcal{E}}]\psi(\bar{z}_{\rm rel}, \varphi_e, \varphi_h) = 0, \tag{A5}$$

which the matrix elements of its potential expression, $V^m_{l_1,l_2}$, is given by

$$V^m_{l_1,l_2}(\chi) = -\frac{2}{\pi\sqrt{\bar{\rho}_e\bar{\rho}_h}} Q_{|m|-1/2}(\chi) + \mu^*\left[\frac{(l_1+m)^2}{m^*_{e_{xy}}\bar{\rho}_e^2} + \frac{(l_2-m)^2}{m^*_{h_{xy}}\bar{\rho}_h^2}\right]\delta_{m,0}, \tag{A6}$$

with $\bar{\rho}_i = \rho_i/a^*$ for $i = e, h$. These matrix elements are equal along each codiagonal in the space spanned by l_1 and l_2. More importantly, the potential matrix has even parity so the functions $f^n_{l_1,l_2}(\bar{z}_{\rm rel})$ of the eigenvectors are either all symmetric or antisymmetric. In Fig. 7, the first nine elements of the matrix $V^m_{l_1,l_2}(z_{\rm rel})$ are depicted as functions of $z_{\rm rel}$ for the case $l=0$. The components $V^m_{l_1,l_2}$ are finite for $z_{\rm rel}=0$ and $Q_{|m|-1/2}(\chi)$ have $-1/\bar{z}_{\rm rel}$ asymptotic behavior for $\bar{z}_{\rm rel} \to \infty$.

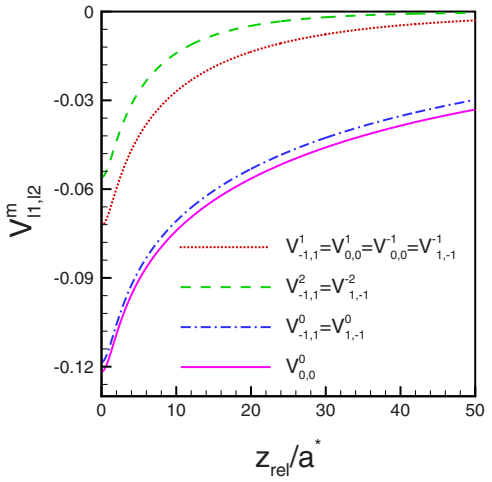

FIG. 7. (Color online) Plots of the first nine components of $V^m_{l_1,l_2}$ as functions of the axial electron-hole separation, $z_{\rm rel}$, for $\rho_h=25a^*$, $\rho_e=26.5a^*$, $d=1.5a^*$, and $l=0$.

APPENDIX B

The constants C_i and the variables of the Legendre function of the second kind, χ_i, for $i=1,2,3,4$ are $C_1=e^2/\pi\varepsilon\rho_e$, $C_2=e^2/\pi\varepsilon\rho_h$, and $C_3=C_4=-e^2/\pi\varepsilon\sqrt{\rho_e\rho_h}$, and $\chi_1=1+(\Delta/a^*)^2+z_1^2/2\rho_e^2$, $\chi_2=1+(\Delta/a^*)^2+z_2^2/2\rho_h^2$, $\chi_3=(\rho_e^2+\rho_h^2+z_3^2)/2\rho_e\rho_h$, and $\chi_4=(\rho_e^2+\rho_h^2+z_4^2)/2\rho_e\rho_h$, where $z_1=z+(z_{\rm rel_1}-z_{\rm rel_2})m^*_{h_z}/M^*$, $z_2=z-(z_{\rm rel_1}-z_{\rm rel_2})m^*_{e_z}/M^*$, $z_3=z+(m^*_{h_z}z_{\rm rel_1}+m^*_{e_z}z_{\rm rel_2})/M^*$, and $z_4=-z+(m^*_{e_z}z_{\rm rel_1}+m^*_{h_z}z_{\rm rel_2})/M^*$. The constant $\Delta=10^{-5}a^*$ is the classical radius of electron, introduced into the potential to prevent the *e-e* and *h-h* Coulomb interactions from diverging at $z_1=0$ and $z_2=0$.

For considering the asymptotic behavior of the functions $Q_{|m|-1/2}(\chi_i)$, we express them in terms of Gauss's hypergeometric functions, as follows:

$$Q_{|m|-1/2}(\chi_i)=\frac{\sqrt{\pi}\Gamma\left(\frac{2m+1}{2}\right)}{\Gamma(m+1)(2\chi_i)^{2m+1/2}}{}_2F_1\left(\frac{2m+3}{4},\frac{2m+1}{4};m+1;\frac{1}{\chi_i^2}\right);\quad i=1,2,3,4, \tag{B1}$$

where Γ is the Gamma function and ${}_2F_1$ is the specific hypergeometric function.[45] Using the series expansion for ${}_2F_1$, we obtain the following expression for $Q_{-1/2}(\chi_i)$

$$Q_{-1/2}(\chi_i)=\frac{\Gamma\left(\frac{1}{2}\right)\sqrt{\pi}}{\Gamma\left(\frac{3}{4}\right)\Gamma\left(\frac{1}{4}\right)(2\chi_i)^{1/2}}\sum_{n=0}^{\infty}\frac{\Gamma\left(\frac{4n+3}{4}\right)\Gamma\left(\frac{4n+1}{4}\right)}{[\Gamma(n+1)]^2\chi_i^{2n}};$$

$$i=1,2,3,4. \tag{B2}$$

Upon evaluating the limit of $C_iQ_{-1/2}(\chi_i)$ for large values of z, $z\gg\rho_e$, to the order of $1/|\bar{z}|^6$ in terms of dimensionless variables, we obtain

$$\begin{aligned}\lim_{\bar{z}\to\infty}\left(\sum_{i=1}^{4}C_iQ_{-1/2}(\chi_i)\right)&=2(-A_1-A_2+A_3+A_4)\left(\frac{1}{|\bar{z}|}\right)^2+2\left[\left(A_1^2-\frac{1}{2B_1}\right)+\left(A_2^2-\frac{1}{2B_2}\right)-\left(A_3^2-\frac{U}{2B}\right)-\left(A_4^2-\frac{U}{2B}\right)\right]\left(\frac{1}{|\bar{z}|}\right)^3\\&+2\left[\left(-A_1^3+\frac{3A_1}{2B_1}\right)+\left(-A_2^3+\frac{3A_2}{2B_2}\right)-\left(-A_3^3+\frac{3A_3U}{2B}\right)-\left(A_4^3-\frac{3A_4U}{2B}\right)\right]\left(\frac{1}{|\bar{z}|}\right)^4\\&+2\left[\left(A_1^4-\frac{3A_1^2}{B_1}+\frac{3}{8B_1^2}\right)+\left(A_2^4-\frac{3A_2^2}{B_2}+\frac{3}{8B_2^2}\right)-\left(A_3^4-\frac{3UA_3^2}{B}+\frac{3U^2}{8B^2}\right)\right.\\&\left.-\left(A_4^4-\frac{3UA_4^2}{B}+\frac{3U^2}{8B^2}\right)-\frac{3}{8B^2}+\frac{3}{16B_1^2}+\frac{3}{16B_2^2}\right]\left(\frac{1}{|\bar{z}|}\right)^5+O\left(\frac{1}{|\bar{z}|}\right)^6,\end{aligned} \tag{B3}$$

in which $A_1=(\bar{z}_{\rm rel_1}-\bar{z}_{\rm rel_2})m^*_{h_z}/M^*$, $A_2=-(\bar{z}_{\rm rel_1}-\bar{z}_{\rm rel_2})m^*_{e_z}/M^*$, $A_3=(m^*_{h_z}\bar{z}_{\rm rel_1}+m^*_{e_z}\bar{z}_{\rm rel_2})/M^*$, $A_4=(m^*_{e_z}\bar{z}_{\rm rel_1}+m^*_{h_z}\bar{z}_{\rm rel_2})/M^*$, $B_1=1/2\bar{\rho}_e^2$, $B_2=1/2\bar{\rho}_h^2$, $B=1/2\bar{\rho}_e\bar{\rho}_h$, and $U=\frac{\bar{\rho}_e^2+\bar{\rho}_h^2}{2\bar{\rho}_e\bar{\rho}_h}$. In Eq. (B3) only those terms, which have even parity over $z_{\rm rel_1}$ and $z_{\rm rel_2}$, contribute to the interaction potential between two excitons. Owing to the odd symmetry, it can be easily verified that the first three terms do not have any quota. Therefore, only the even-parity terms in the coefficient of the quadrupole term, i.e., the fourth term, has significant contribution. By dropping terms that have odd parity, the coefficient of the quadrupole term simplifies to

$$C_{\rm quad}=12\left(\frac{m^{*^2}_{e_z}-m^{*^2}_{h_z}}{M^{*^2}}\right)^2\bar{z}^2_{\rm rel_1}\bar{z}^2_{\rm rel_2}+6\left(\frac{m^{*^2}_{e_z}+m^{*^2}_{h_z}}{M^{*^2}}\right)(\bar{\rho}_e^2-\bar{\rho}_h^2)\times(\bar{z}^2_{\rm rel_1}-\bar{z}^2_{\rm rel_2})+3(\bar{\rho}_e^2-\bar{\rho}_h^2)^2. \tag{B4}$$

Using Eq. (11) the repulsive quadrupole interaction between

two excitons can then be written as follows:

$$\mathbf{V}(|\bar{z}|) = \frac{M_{\text{quad}}}{|\bar{z}|^5}, \tag{B5}$$

where M_{quad} is given by

$$M_{\text{quad}} = \int_{-\infty}^{\infty}\int_{-\infty}^{\infty} d\bar{z}_{\text{rel}_1} d\bar{z}_{\text{rel}_2} C_{\text{quad}}(\bar{z}_{\text{rel}_1}, \bar{z}_{\text{rel}_2}) \sum_{\mu=-52}^{52} \sum_{\mu'=-52}^{52} |f^0_{\mu,-\mu}(\bar{z}_{\text{rel}_1})|^2 |f^0_{\mu',-\mu'}(\bar{z}_{\text{rel}_2})|^2, \tag{B6}$$

which is equal to

$$M_{\text{quad}} = 12\left(\frac{m^{*2}_{e_z} - m^{*2}_{h_z}}{M^{*2}}\right)^2 \bar{a}^4 + 3(\bar{\rho}_e^2 - \bar{\rho}_h^2)^2. \tag{B7}$$

*mh-bagheri@cc.sbu.ac.ir
†ebrahimi@sbu.ac.ir

[1] M. H. Anderson, J. R. Ensher, M. R. Matthews, C. E. Wieman, and E. A. Cornell, Science **269**, 198 (1995).
[2] A. J. Leggett, *Quantum Liquids: Bose Condensation and Cooper Pairing in Condensed-Matter Systems* (Oxford University Press, New York, 2006).
[3] S. A. Moskalenko and D. W. Snoke, *Bose-Einstein Condensation of Excitons and Biexcitons* (Cambridge University Press, Cambridge, 2000).
[4] W. Ketterle, Rev. Mod. Phys. **74**, 1131 (2002).
[5] D. Snoke, Science **298**, 1368 (2002).
[6] L. V. Butov, A. C. Gossard, and D. S. Chemla, Nature (London) **418**, 751 (2002).
[7] C. W. Lai, J. Zoch, A. C. Gossard, and D. S. Chemla, Science **303**, 503 (2004).
[8] V. Savona and D. Sarchi, Phys. Status Solidi B **242**, 2290 (2005).
[9] P. B. Littlewood, P. R. Eastham, J. M. J. Keeling, F. M. Marchetti, B. D. Simons, and M. H. Szymanska, J. Phys.: Condens. Matter **16**, S3597 (2004).
[10] J. Kasprzak, M. Richard, S. Kundermann, A. Baas, P. Jeambrun, J. M. J. Keeling, F. M. Marchetti, M. H. Szymaska, R. André, J. L. Staehli, V. Savona, P. B. Littlewood, B. Deveaud, and Le Si Dang, Nature (London) **443**, 409 (2006).
[11] S. O. Demokritov, V. E. Demidov, O. Dzyapko, G. A. Melkov, A. A. Serga, B. Hillebrands, and A. N. Slavin, Nature (London) **443**, 430 (2006).
[12] J. P. Eisenstein and A. H. Macdonald, Nature (London) **432**, 691 (2004).
[13] S. A. Moskalenko, Sov. Phys. Solid State **4**, 199 (1962).
[14] J. M. Blatt, K. W. Böer, and W. Brandt, Phys. Rev. **126**, 1691 (1962).
[15] L. V. Keldysh and A. N. Kozlov, Sov. Phys. JETP **27**, 521 (1968).
[16] N. Peyghambarian, L. L. Chase, and A. Mysyrowicz, Phys. Rev. B **27**, 2325 (1983).
[17] D. W. Snoke, J. P. Wolfe, and A. Mysyrowicz, Phys. Rev. Lett. **64**, 2543 (1990).
[18] D. W. Snoke, J. L. Lin, and J. P. Wolfe, Phys. Rev. B **43**, 1226 (1991).
[19] E. Fortin, S. Fafard, and A. Mysyrowicz, Phys. Rev. Lett. **70**, 3951 (1993).
[20] M. Hasuo, N. Nagasawa, T. Itoh, and A. Mysyrowicz, Phys. Rev. Lett. **70**, 1303 (1993).
[21] Yu. E. Lozovik and V. I. Yudson, Sov. Phys. JETP **44**, 389 (1976).
[22] T. Fukuzawa, E. E. Mendez, and J. M. Hong, Phys. Rev. Lett. **64**, 3066 (1990).
[23] X. Zhu, P. Littlewood, M. Hybertsen, and T. Rice, Phys. Rev. Lett. **74**, 1633 (1995).
[24] L. V. Butov, A. Zrenner, G. Abstreiter, G. Böhm, and G. Weimann, Phys. Rev. Lett. **73**, 304 (1994); L. V. Butov, Solid State Commun. **127**, 89 (2003); L. V. Butov, J. Phys.: Condens. Matter **16**, R1577 (2004).
[25] S. De Palo, F. Rapisarda, and G. Senatore, Phys. Rev. Lett. **88**, 206401 (2002).
[26] D. Snoke, S. Denev, Y. Liu, L. Pfeiffer, and K. West, Nature (London) **418**, 754 (2002).
[27] L. V. Keldysh and Y. V. Kopaev, Sov. Phys. Solid State **6**, 2219 (1965); R. R. Gusejnov and L. V. Keldysh, Sov. Phys. JETP **36**, 1193 (1972).
[28] W. Kohn and D. Sherrington, Rev. Mod. Phys. **42**, 1 (1970).
[29] H. Haug and E. Hanamura, Phys. Rev. B **11**, 3317 (1975).
[30] Yu. E. Lozovik and V. I. Yudson, JETP Lett. **22**, 271 (1975); Yu. E. Lozovik and V. I. Yudson, Sov. Phys. Solid State **18**, 1142 (1976); I. V. Lerner and Yu. E. Lozovik, JETP Lett. **27**, 467 (1978); I. V. Lerner and Yu. E. Lozovik, Sov. Phys. JETP **53**, 763 (1981).
[31] D. Jérome, T. M. Rice, and W. Kohn, Phys. Rev. **158**, 462 (1967).
[32] S. I. Shevchenko, Sov. J. Low Temp. Phys. **2**, 251 (1976).
[33] O. G. Schmidt, C. Deneke, Y. M. Manz, and C. Müller, Physica E (Amsterdam) **13**, 969 (2002).
[34] Yu. E. Lozovik and O. L. Berman, JETP **84**, 1027 (1997); Yu. E. Lozovik, O. L. Berman, and M. Willander, J. Phys.: Condens. Matter **14**, 12457 (2002).
[35] L. V. Butov and A. I. Filin, Phys. Rev. B **58**, 1980 (1998).
[36] T. Iida and M. Tsubota, Phys. Rev. B **60**, 5802 (1999).
[37] J. D. Jackson, *Classical Electrodynamics* (Wiley, New York, 1999).
[38] A. G. Abrashkevich and D. G. Abrashkevich, Comput. Phys. Commun. **113**, 105 (1998).
[39] A. L. Fetter and J. D. Walecka, *Quantum Theory of Many-Particle Systems* (McGraw-Hill, New York, 1971).
[40] M. Razavy, *Quantum Theory of Tunneling* (World Scientific,

Singapore, 2003).
[41] M. Olshanii, Phys. Rev. Lett. **81**, 938 (1998).
[42] W. H. Butler, Phys. Rev. B **14**, 468 (1976).
[43] L. Tonks, Phys. Rev. **50**, 955 (1936); M. Girardeau, J. Math. Phys. **1**, 516 (1960).
[44] I. Bouchoule, K. V. Kheruntsyan, and G. V. Shlyapnikov, Phys. Rev. A **75**, 031606(R) (2007); K. V. Kheruntsyan, D. M. Gangardt, P. D. Drummond, and G. V. Shlyapnikov, Phys. Rev. Lett. **91**, 040403 (2003); K. V. Kheruntsyan, D. M. Gangardt, P. D. Drummond, and G. V. Shlyapnikov, Phys. Rev. A **71**, 053615 (2005); D. M. Gangardt and G. V. Shlyapnikov, New J. Phys. **5**, 79 (2003).
[45] H. S. Cohl and J. E. Tohline, Astrophys. J. **527**, 86 (1999); H. S. Cohl, A. R. P. Rau, J. E. Tohline, D. A. Browne, J. E. Cazes, and E. I. Barnes, Phys. Rev. A **64**, 052509 (2001).